TOWARDS A COMPACT MODEL FOR SCHOTTKY-BARRIER NANOTUBE FETS

L.C. Castro, D.L. John and D.L. Pulfrey

Department of Electrical and Computer Engineering
University of British Columbia
Vancouver, BC V6T 1Z4, Canada
contact: pulfrey@ece.ubc.ca

ABSTRACT

Issues pertinent to the development of a compact model for predicting the drain current-voltage characteristics of coaxial-geometry, Schottky-barrier, carbon-nanotube field-effect transistors are discussed. Information on the non-equilibrium barrier shapes at the source-tube and drain-tube contacts is inferred from exact 2-D solutions to Poisson's equation at equilibrium and Laplace's equation. This information is then used in a non-equilibrium flux approach to create a model that accounts for tunneling through both barriers and computes the drain current in the case of ballistic transport. For (16,0) tubes and a gate/tube-radius ratio of 10, saturation drain currents of about $1\,\mu A$ are predicted.

1. INTRODUCTION

Nanoscale transistors fashioned from carbon nanotubes are an exciting possibility [1, 2]. Transport is essentially one-dimensional, and there is very little carrier-phonon interaction [3]. Thus, the drain current tends to be controlled by modulation of the Schottky-barrier potential profiles at the source and drain ends of the nanotube [4, 5, 6]. Present experimental devices are planar in nature [4], but coaxial structures offer better opportunities for modulating the Schottky-barrier properties via capacitative coupling between the gate and the contacts [7, 8]. In the present work we concentrate on coaxial, Schottky-barrier devices formed with intrinsic nanotubes, and seek to develop a compact model for the prediction of the drain *I*-*V* characteristics. The basic transistor structure is shown in Fig. 1.

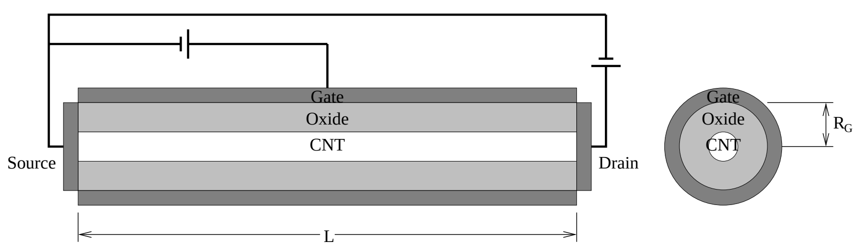

Figure 1: Schottky-barrier, carbon nanotube, FET model geometry (not to scale). The gate forms the curved surface of the outer cylinder, and the source and drain form the two ends. The semiconducting nanotube is placed coaxially with the outer cylinder.

Under equilibrium conditions, which in these devices means no drain current, *i.e.*, the drain-source voltage $V_{DS} = 0$, but the gate-source voltage V_{GS} is not necessarily zero, it is straightforward to compute the charge and potential profile by solving Poisson's equation consistently with the equilibrium charge density on the nanotube [6]. For $V_{GS} > 0$, as considered in this work, the charge on the tube is negative, and is due to a surfeit of electrons over holes. Here we take the electronic charge to dominate and we neglect the contribution of the holes. Away from equilibrium, when $V_{DS} > 0$, the induced electron distribution on the tube will deviate considerably from a Maxwellian or Fermi-Diracian form, on account of hot electron injection from the contacts and, in the ballistic case considered here, the lack of opportunity for thermalizing collisions. This precludes the calculation of the non-equilibrium charge using simple, quasi-Fermi-Dirac statistics.

In the present work, we obtain an estimate of the non-equilibrium charge Q_C in the mid-length region of the tube, *i.e.*, away from the source and drain potential barriers, by an extension of the method of Guo *et al.* [9, 10]. Q_C is related to the mid-length potential on the tube V_{CS}, which connects, and affects, the potential profiles of the Schottky barriers. These, in turn, affect the tunneling probabilities for electrons entering the tube from the reservoirs of equilibrium charge at the source and drain metallizations. The energy-dependent tunneling probabilities serve to distort the electron distribution in the tube from an equilibrium form. Here, we take the potential profiles at the barriers to have an exponential form, and then solve for V_{CS} by equating the values of Q_C computed by the non-equilibrium-flux approach and an infinite-tube approach [9, 10]. This gives a solution to the complete potential profile, and to the tunneling probabilities, which then allows computation of the drain current from Landauer's expression. Our inclusion of the Schottky-barrier nature of the contacts leads to a significantly different saturation current than predicted by the earlier model [9], in which the tunneling barriers were not considered.

2. THE MODEL

At equilibrium, *i.e.*, when $V_{DS} = 0$, simple electrostatics gives:

$$\tilde{Q}_C = -C_\infty(V_{GS} - \tilde{V}_{CS}) \;, \tag{1}$$

where $\tilde{V}_{CS}$ is the equilibrium potential, with respect to the source, of the carbon nanotube at its mid-length, *i.e.*, away from the influence of the source and drain contacts, and C_∞ is the insulator capacitance for an infinitely long coaxial system. Out of equilibrium, *i.e.*, when $V_{DS} \neq 0$, V_{CS} is influenced by V_{DS}:

$$\begin{aligned} V_{CS} &= \tilde{V}_{CS} + \alpha V_{DS} && (2)\\ Q_C &= -C_\infty(V_{GS} - V_{CS}) \;, && (3) \end{aligned}$$

where α is a parameter that needs to be determined in order to specify V_{CS}. For $V_{GS} > 0$, as considered in this work, Q_C is a negative, electronic charge.

An alternative method for calculating Q_C follows from the flux approach, in which electrons in the forward- and backward-directed fluxes are summed [9]. Here, we do not restrict the fluxes within the tube to be hemi-Maxwellian or hemi-Fermi-Diracian in nature, but, instead, we allow the actions of tunneling and repeated reflections between the potential barriers to modify the electron distributions from the equilibrium form that they possess outside the tube, at the actual source and drain metallic contacts. In the following, f_S^+ denotes the positive- or forward-directed part of the Fermi-Dirac distribution outside the tube at the source, whereas f_D^- represents the negative- or backward-directed part of the distribution outside the tube at the drain. Thus:

$$\begin{aligned} Q_C = -q\Bigg\{&\int_{E_C}^{\infty} g(E) f_S^+(E)\left(\frac{2}{T_D}-1\right)T^*\,dE \\ &+\int_{E_C}^{\infty} g(E) f_D^-(E,V_{DS})\left(\frac{2}{T_S}-1\right)T^*\,dE\Bigg\} \;, \end{aligned} \tag{4}$$

where $g(E)$ is the 1-D density of states computed from the tight-binding approximation [11], the conduction band edge E_C in the mid-length region of the tube is dependent on αV_{DS}, and the tunneling probabilities at the source and drain, T_S and T_D respectively, are computed using the JWKB approximation and are dependent on E, V_{GS} and αV_{DS}. The overall transmission probability $T^* = T_S T_D/(T_S + T_D - T_S T_D)$. In our method, we equate (3) and (4) and solve for α, thereby determining V_{CS}. An iterative procedure is necessary because of the dependence on V_{CS} of T_S and T_D, via the potential profile, which is represented by

$$V(z) = \begin{cases} V_{CS} - \frac{V_{CS}}{e^{\beta}-1}\left[e^{-\frac{\beta}{a}(z-a)} - 1\right] & 0 \le z \le a \\ V_{CS} & a \le z \le L-a \\ V_{CS} - \frac{V_{CS}-V_{DS}}{e^{\beta}-1}\left[e^{-\frac{\beta}{a}(L-a-z)} - 1\right] & L-a \le z \le L \end{cases} \tag{5}$$

where z is the distance from the source and L is the tube length. This representation is based on observation of the trends in barrier shape under those circumstances for which exact solutions are presently possible, namely:

Poisson's equation at equilibrium, and Laplace's equation out of equilibrium. The trends are: a barrier base-width of $a \approx 2R_G$, where R_G is the radius of the gate (see Fig. 1); a barrier height at the source of $V_{pk} = V_{CS}$ (see Fig. 2); a barrier height at the drain that varies from $V_{pk} = V_{CS} - V_{DS}$ when a "spike" is present, through $V_{pk} = 0$, to a negative value when $V_{DS} > V_{CS}$ (see Fig. 2); a barrier "concavity" that is captured by $\beta \approx 3.6$ for the tube considered here. The barrier profiles given by (5) are correct inasmuch as they prescribe values for the tunneling probabilities T_S and T_D that yield a mid-length charge that is consistent with that predicted by (3).

To complete the calculation of the drain current, the Landauer expression is used:

$$I_D = \sum_i \frac{2q}{\pi\hbar} \int_{E_{Ci}}^{\infty} \left[f_S^+(E) - f_D^-(E, V_{DS}) \right] T^* \, dE \,, \tag{6}$$

where the sum is over the i conduction bands, the edges E_{Ci} of which are functions of α, V_{GS} and V_{DS}.

3. RESULTS AND DISCUSSION

Results are presented for a (16,0) tube, which has a radius of 0.63 nm, and a gate/tube-radius ratio of 10; the source and drain work functions are taken to be equal to that of the intrinsic nanotube. The tube is sufficiently long that there is a "mid-length" region where the tube potential V_{CS} is flat. In this region, we have found that there is essentially perfect agreement between the values of V_{CS} calculated by the "infinite-tube" method (1), and by an exact 2-D solution [6], at least under the equilibrium conditions tested thus far. The energy band diagram for a variety of bias conditions is shown in Fig. 2. Note the V_{DS}-dependence of V_{CS} and of the barrier shapes.

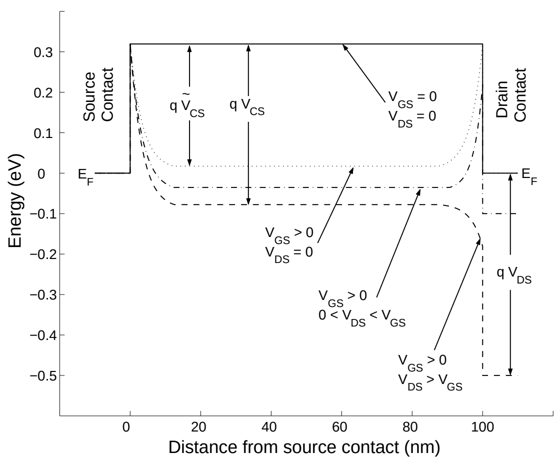

Figure 2: Conduction energy band diagram for various bias conditions.

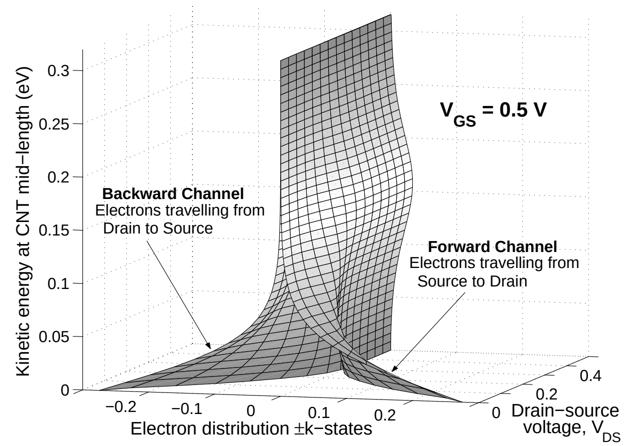

Figure 3: Electron distribution in the "mid-length" of the tube as a function of V_{DS} for $V_{GS} = 0.5\,\mathrm{V}$.

Electrons from the source and drain reservoirs are drawn into the tube by tunneling through, and thermionic emission over, the potential barriers at the contacts. This distorts the injected electron distributions from their equilibrium forms. The total distribution within the tube is determined by the action of reflections at the Schottky barriers on the injected distributions. When $V_{DS} = 0$ this action produces an equilibrium, Fermi-Dirac distribution, as can be seen in Fig. 3. As V_{DS} increases, there is less injection from the drain, and less reflection from the diminishing "spike" at the drain. Thus, the backward-directed part of the distribution starts to disappear, and the forward part assumes a definitely non-equilibrium shape, with a bulge at the kinetic energy corresponding to that of the maximum tunneling flux.

The drain I-V characteristics are shown in Fig. 4. The saturation current at $V_{GS} = 0.5\,\mathrm{V}$ is around $1\,\mu A$, which is not inconsistent with values emerging from prototype devices [12]. A revealing comparison with

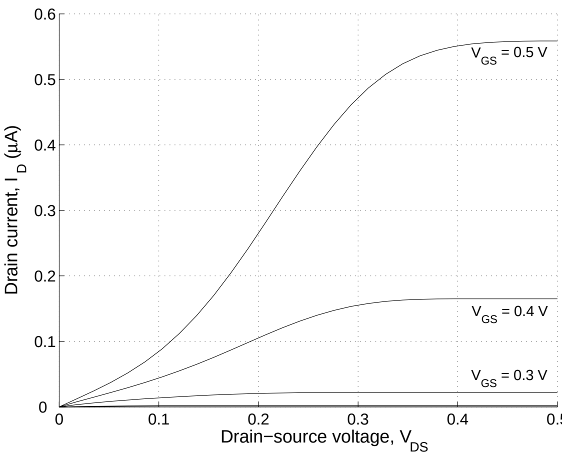

Figure 4: Drain current-voltage characteristics.

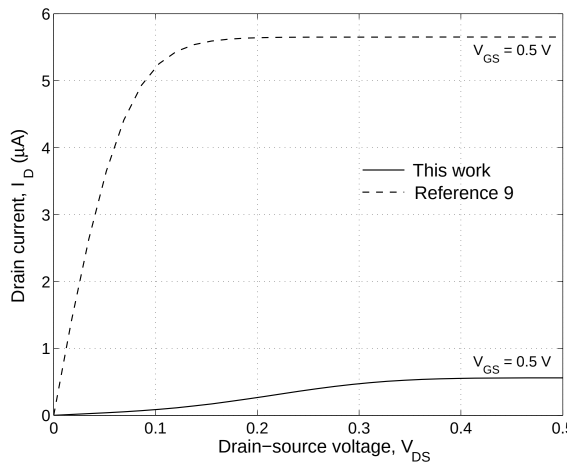

Figure 5: Comparison of drain current-voltage characteristics at $V_{GS} = 0.5\,\mathrm{V}$. The solid line is this work; the dashed line is using the model of Ref. [9].

earlier predictions is shown in Fig. 5. Note how the present model indicates a considerably larger saturation voltage $V_{DS,sat}$. This is because the reflecting action of the potential "spike" at the tube-drain interface delays the realization of the full saturation current. Also, note how the new model predicts an $I_{D,sat}$ that is about one-order of magnitude less than that of the model of Guo *et al.* [9]. This is indicative of the importance of accounting for the restrictive action that the Schottky barriers at the source and drain impose on the current.

4. CONCLUSIONS

From this work on the modeling of coaxial, carbon nanotube FETs, it can be concluded that the Schottky barriers at the source and drain contacts play a dominant role in determining the *I-V* characteristics of the transistors. The model presented here represents a significant step towards producing a compact model for these promising new nano-devices.

References

[1] V. Derycke, R. Martel, J. Appenzeller, and Ph. Avouris, *Nano Lett.*, **1**(9), 453 (2001).

[2] A. Bachtold, P. Hadley, T. Nakanishi, and C. Dekker, *Science*, **294**, 1317 (2001).

[3] P.L. McEuen, M.S. Fuhrer, and H. Park, *IEEE Trans. Nanotechnology*, **1**(1), 78 (2002).

[4] J. Appenzeller, J. Knoch, V. Derycke, R. Martel, S. Wind, and Ph. Avouris, *Phys. Rev. Lett.*, **89**(12), 126801 (2002).

[5] S. Heinze, J. Tersoff, R. Martel, V. Derycke, J. Appenzeller, and Ph. Avouris, *Phys. Rev. Lett.*, **89**(10), 106801 (2002).

[6] D.L. John and D.L. Pulfrey, *Appl. Phys. Lett.*, submitted August 2002.

[7] C.P. Auth and J.D. Plummer, *IEEE Electron Dev. Lett.*, **18**(2), 74 (1997).

[8] B. Winstead and U. Ravaioli, *IEEE Trans. Electron Devices*, **47**(6), 1241 (2000).

[9] J. Guo, M. Lundstrom, and S. Datta, *Appl. Phys. Lett.*, **80**(17), 3192 (2002).

[10] J. Guo, S. Goasguen, M. Lundstrom, and S. Datta, *Appl. Phys. Lett.*, **81**(8), 1486 (2002).

[11] K. Esfarjani, A.A. Farajian, Y. Hashi, and Y. Kawazoe, in *Clusters and Nanomaterials—Theory and Experiment*, edited by Y. Kawazoe, T. Kondow, and K. Ohno, (Springer-Verlag, Berlin, 2002), Chap. 8, pp. 187–220.

[12] S. Rosenblatt, Y. Yaish, J. Park, J. Gore, V. Sazonova, and P.L. McEuen, *Nano Lett.*, **2**(8), 869 (2002).